International Journal of Science and Research Archive

eISSN: 2582-8185

Cross Ref DOI: 10.30574/ijsra

Journal homepage: https://ijsra.net/

(RESEARCH ARTICLE)

Check for updates

Elucidating the Electronic and Structural Properties of Cu_2MgSnS_4 through Density Functional Theory

G. Somasundari *

Department of Chemistry, Grace College of Engineering, Thoothukudi, Tamilnadu -628005, India.

International Journal of Science and Research Archive, 2025, 14(03), 1354-1361

Publication history: Received on 07 February 2025; revised on 18 March 2025; accepted on 21 March 2025

Article DOI: https://doi.org/10.30574/ijsra.2025.14.3.0741

Abstract

In this study, a comprehensive density functional theory calculation is done to investigate the electronic and optical properties of Cu_2MgSnS_4, assessing its viability as absorber materials for photovoltaic applications. Analysis indicates that traditional approaches using the modified Becke-Johnson (mBJ) potential, similar to the General Gradient Approximation (GGA) and Local Density Approximation (LDA), do not accurately predict the experimental bandgap values, underscoring the limitations of the TB-mBJ potential for semiconductors with strongly delocalized d-electrons. To overcome this the mBJ potential is integrated with the Hubbard U correction (mBJ + U) to enhance the representation of pd hybridization and achieving a computed bandgap of 1.49 eV. Cu_2MgSnS_4 exhibit high optical absorption coefficients exceeding 10^4 cm^{-1} in the visible spectrum and lower reflectivity compared to silicon, suggesting a potential for superior solar cell performance due to enhanced light absorption capabilities.

Keywords: First-principles calculations; Quaternary Chalcogenide; Kesterite; Stannite; Cu_2MgSnS_4

1. Introduction

As the global demand for energy continues to rise and fossil fuel resources become increasingly scarce, large-scale solar energy production is expected to play a crucial role in meeting future energy needs. Solar energy is an abundant and sustainable resource that does not contribute to harmful emissions, making it an environmentally friendly alternative. The quaternary semiconductor Cu_2ZnSnS_4 (CZTS) has garnered significant attention from researchers and laboratories worldwide as a promising candidate for solar absorber materials [1–4]. CZTS exhibits electronic and optical properties well-suited for photovoltaic applications, including a direct band gap of approximately 1.4 to 1.5 eV [5,6], which is ideal for achieving high single-junction solar cell efficiency. Additionally, CZTS possesses a large absorption coefficient in the visible wavelength region [7], making it an excellent choice for thin-film solar cells. This high absorption capability allows for reduced material usage, leading to lower production costs.

Furthermore, CZTS is composed of non-toxic, earth-abundant, and cost-effective elements, making large-scale production feasible. Over the past years, the conversion efficiency of CZTS-based solar cells has shown continuous improvement. Pure sulfide CZTS solar cells have achieved a conversion efficiency of 8.4% [8], while mixed sulfide-selenide $Cu_2ZnSn(S,Se)_4$ absorber layers have reported efficiencies as high as 12% [9]. These advancements highlight the potential of CZTS-based materials for next-generation photovoltaic applications.

Extensive research and development efforts on $Cu_2ZnSn(S,Se)_4$ (CZTSSe) are being conducted worldwide, with a significant focus on understanding defects within the material [10–17]. In addition to CZTSSe, researchers have explored similar quaternary compounds by substituting Zn with transition metal atoms such as Mn, Fe, Co, and Ni.

* Corresponding author: G. Somasundari

Copyright © 2025 Author(s) retain the copyright of this article. This article is published under the terms of the Creative Commons Attribution Liscense 4.0.

For instance, the fundamental band-gap energy (*Eg*) of Cu_2MnSnS_4 has been experimentally estimated to range between 1.18 and 1.63 eV, depending on heat treatment conditions [18]. A solar cell based on Cu_2MnSnS_4 has demonstrated an efficiency of 0.49%. The band-gap energies of synthesized Cu_2FeSnS_4 nanocrystals and Cu_2CoSnS_4 and Cu_2NiSnS_4 nanoparticles have been reported as approximately 1.33–1.5 eV [19,20], 1.40 eV [21], and 1.40 eV [22,5], respectively. Additionally, kesterite Cu_2MgSnS_4 nanoparticles have been successfully synthesized without secondary phases using a hot-injection method [23].

First-principles calculations based on the generalized gradient approximation (GGA) by Wang et al. [24] indicate that kesterite Cu_2CdSnS_4 and Cu_2HgSnS_4 are thermodynamically stable, whereas kesterite Cu_2MgSnS_4 and, more notably, Cu_2CaSnS_4 are not. Complementary findings by Zhong et al. [25] using hybrid functional calculations suggest that stannite Cu_2MgSnS_4 and $Cu_2MgSnSe_4$ are thermodynamically stable, while both kesterite and stannite phases of Cu_2CaSnS_4 and $Cu_2CaSnSe_4$ are unstable due to competition with other compounds. Some of these alternative compounds hold potential as thin-film photovoltaic materials. However, further advancements in synthesis techniques and a deeper understanding of native defect impacts are necessary to optimize their performance and viability for large-scale solar energy applications. Cu_2MgSnS_4 (Copper Magnesium Tin Sulfide) is a quaternary chalcogenide compound composed of copper (Cu), magnesium (Mg), tin (Sn), and sulfur (S). It belongs to the I_2-II-IV-VI_4 family of materials, which are structurally similar to kesterites like Cu_2ZnSnS_4 (CZTS). The crystal structure of Cu_2MgSnS_4 can exhibit a stannite-like or kesterite-like arrangement, depending on synthesis conditions. The electronic properties of Cu_2MgSnS_4 in both kesterite (KS) and stannite (ST) phases were computed using the Wien2k code. The calculations employed the generalized gradient approximation (GGA), the modified Becke–Johnson exchange potential (TB-mBJ), and the Hubbard potential (U) to account for electron interactions.

It was observed that the TB-mBJ potential, similar to GGA and LDA, tends to underestimate the band gap value, highlighting its limitations in semiconductors containing strongly delocalized *d* electrons. To address this issue, the TB-mBJ potential combined with the Hubbard U correction (TB-mBJ+U) was utilized, yielding band gap values more consistent with experimental data. This approach enhances *p-d* hybridization, leading to a more accurate determination of the energy gap (*Eg*) for the stable phases analyzed in this study.

The computational methodology is detailed in Section 2, followed by a discussion on the structural, mechanical, electronic, and optical properties in Section 3. The key findings and conclusions are summarized in Section 4.

2. Computational Details

The structural, electronic, and optical properties of Cu_2MgSnS_4 were investigated using the full-potential linearized augmented plane-wave (FP-LAPW) method implemented in the WIEN2k code [26,27]. The exchange-correlation potential was treated using the generalized gradient approximation (GGA) as formulated by Perdew et al. [28]. Since the local density approximation (LDA) and GGA are known to underestimate the band gap of semiconductors, the modified Becke-Johnson (TB-mBJ) potential [29] was employed to improve the accuracy of band gap calculations. Additionally, the TB-mBJ potential combined with the Hubbard U correction (TB-mBJ+U) was applied to obtain band gap values that are in better agreement with experimental results. For the electronic structure calculations, the valence electron configurations used were as follows: (Cu): $3d^{10}$ $4s^1$, (Mg): $2p^6$ $3s^2$, (Sn): $5s^2$ $5p^2$, (S): $3S^2$ $3P^4$. The muffin-tin (MT) radii were set as follows for different atoms in Cu_2MgSnS_4 are Cu: 2.35, Mg: 2.3, Sn: 2.47, S: 2.25. The plane-wave cut-off parameter ($R_{MT}K_{MAX}$) was set to 7, where R_{MT} is the muffin-tin radius and K_{MAX} represents the plane-wave cut-off. The effective Hubbard U value used was Ueff = U - J = 5 eV. For crystal structure optimization, calculating the density of states (DOS) and optical properties a 10 × 10 × 10 k-mesh was used.

3. Results and Discussion

3.1. Structural properties

Quaternary chalcogenide crystals can exist in five distinct phases: kesterite, wurtzite kesterite, stannite, wurtzite stannite, and primitive-mixed CuAu (PMCA) [30]. Among these, the stannite (ST) and kesterite (KS) phases are thermodynamically stable, with space groups I-42m and I4, respectively. In the kesterite (KS) structure (space group I4), the conventional unit cell comprises: Four Cu atoms positioned at Wyckoff sites 2a and 2c, two Mg atoms at 2d, two Sn atoms at 2b, eight Se atoms at 8g. Conversely, in the stannite (ST) structure (space group I-42m), the unit cell consists of: Four Cu atoms at the 4d position, two Mg atoms at 2a, two Sn atoms at 2b, eight Se atoms at 8i. The crystal structures of the KS and ST phases are illustrated in Figure 1, highlighting the atomic arrangements and symmetry differences between these two stable configurations.

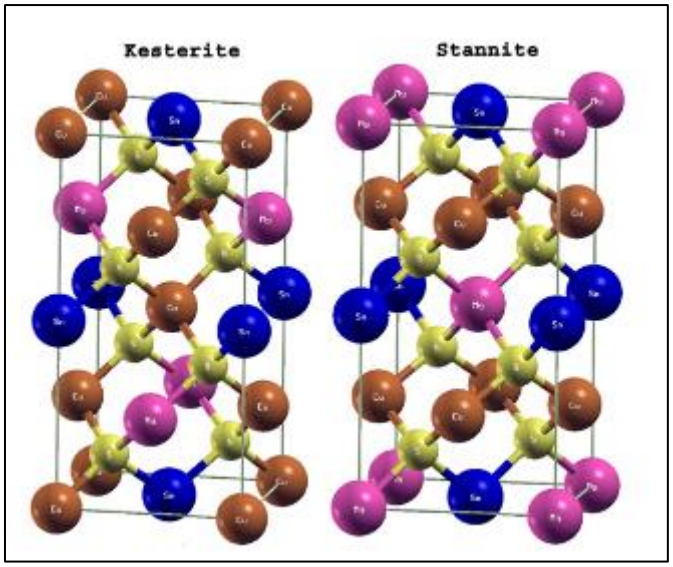

Figure 1 Crystal structure of of Cu_2MgSnS_4 (in kesterite and stannite phases)

The ground-state parameters, including lattice constants (a and c), bulk modulus (B), and its derivative (B'), were determined by plotting the calculated total energy against the equilibrium volume and fitting the data to the empirical Birch-Murnaghan equation [31]. The total energy study reveals that the ST phase is more stable than KS phase.

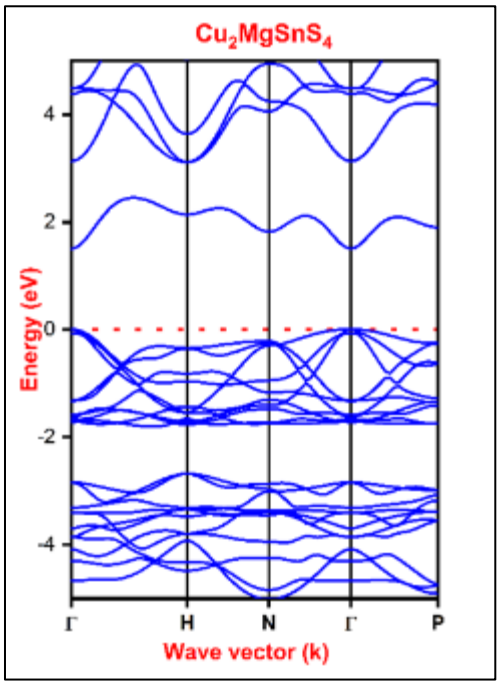

Figure 2 The electronic band structure of Cu_2MgSnS_4.

The lattice constants for the ground-state structure of Cu_2MgSnS_4 are summarized in Table 1.

Table 1 Calculated lattice parameters a(Å) and c(Å), Volume (Å^3), bulk modulus B(GPa) and its derivative B′, Band gap E_g (eV)

Compound	a	c/a	Bo	B'	E_g(eV)	Refractive index	Reflectivity
Cu_2MgSnS_4	5.596	1.960	65.83	3.44	1.49	2.29	0.153

3.2. Electronic properties

The partial density of states (PDOS) and total density of states (TDOS) were computed using the TB-mBJ+U potential to ensure accurate electronic structure predictions. The Cu_2MgSnS_4 compound exhibit a direct band gap, with both the valence band maximum (VBM) and conduction band minimum (CBM) located at the Γ point, as depicted in Figure 2. The band gap value obtained is listed in Table 1, providing essential insights into its suitability for optoelectronic applications.

The partial density of states (PDOS) analysis of Cu_2MgSnS_4 reveals distinct contributions from various atomic orbitals across different energy regions. Total density of states (DOS) and Partial density of states (PDOS) using mBJ + U is shown in Figure 3.

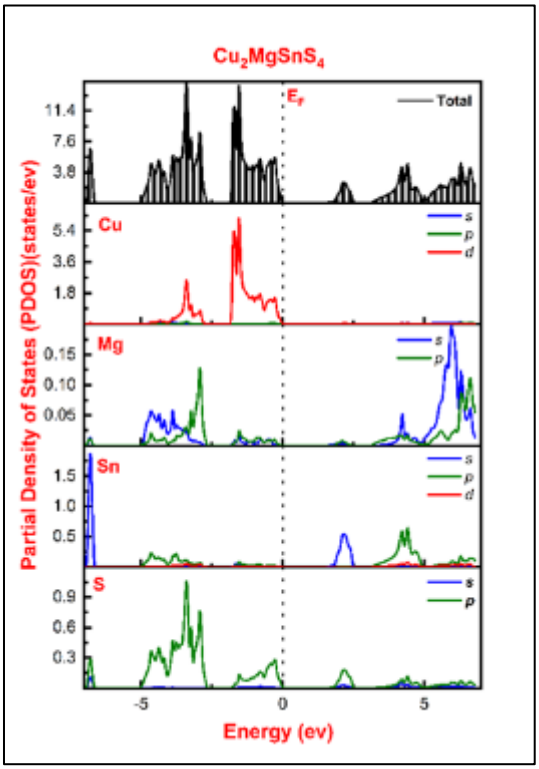

Figure 3 Total density of states (DOS) and Partial density of states (PDOS) of Cu_2MgSnS_4.

The energy range from -5 eV to -2.5 eV is predominantly characterized by the contributions of Cu-3d, Sn-5p, and S-3p states, with minimal influence from Mg states. The region between -2.5 eV and the Fermi level is primarily composed of Cu-3d and S-3p states. The energy range from the Fermi level to 2.5 eV consists of an unfilled anti-bonding orbital formed by the hybridization of Sn-5s, S-3p, and Cu-3d states. The higher energy regions beyond 5 eV are mainly composed of Sn-p, S-p, S-s, and Cu-d states. The valence band maximum (VBM) is predominantly anti-bonding in nature, arising from the hybridization of p orbitals (S-3p) with d orbitals (Cu-3d). Meanwhile, the conduction band minimum (CBM) is primarily composed of anti-bonding states formed by s-s and s-p hybridization between the Sn cation and S anion, with a significant contribution from the Cu-d states. These characteristics play a crucial role in determining the electronic and optical properties of Cu_2MgSnS_4.

3.3. Optical properties

The real and imaginary components of the complex dielectric function, expressed as $\varepsilon(\omega) = \varepsilon_1(\omega) + i\varepsilon_2(\omega)$, were computed using the Kramers-Kronig relations. The real part ($\varepsilon_1(\omega)$) of the dielectric function is directly associated with the electronic dispersion in the material. Figure 4 illustrates the real (dispersive) part of the dielectric function, providing insights into the optical response of the investigated materials.

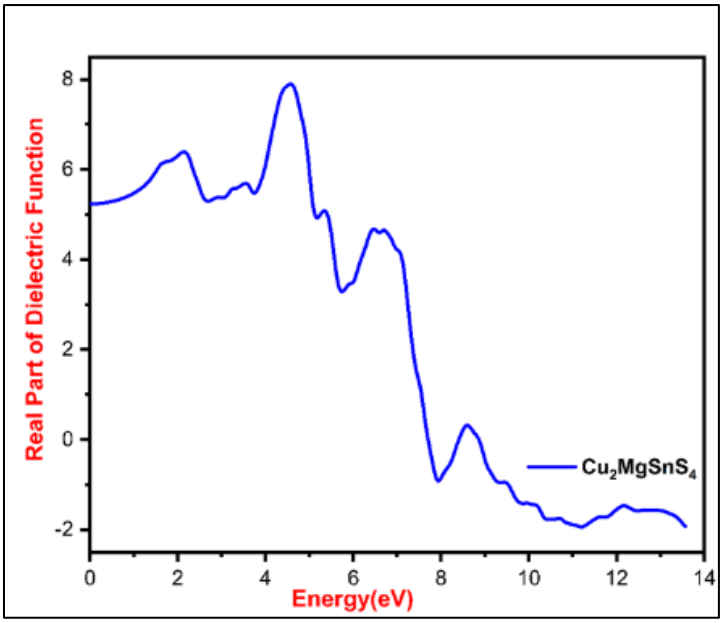

Figure 4 Energy versus dielectric function of of Cu_2MgSnS_4.

The reflectivity represents the ratio of reflected to incident light intensity and is a key parameter in assessing the surface optical properties of materials. As shown in Fig.5**,** the investigated materials exhibit high reflectivity at higher energies, particularly in the visible and UV regions, making them promising candidates for optical applications**.**

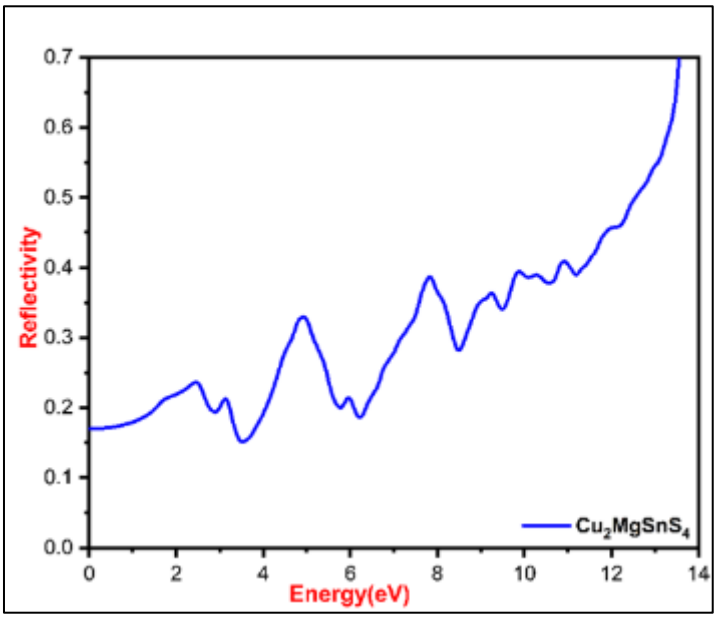

Figure 5 Energy versus reflectivity of Cu_2MgSnS_4 in stable phases

The absorption coefficient determines how deeply light penetrates before being absorbed within the material. This spectral characteristic arises due to interband transitions and is crucial for photovoltaic applications. An ideal photovoltaic material should possess a direct band gap, along with low reflectance and high absorption in the visible spectrum**.** Fig.6 presents the absorption coefficient spectrum, highlighting the material's suitability for light-harvesting applications.

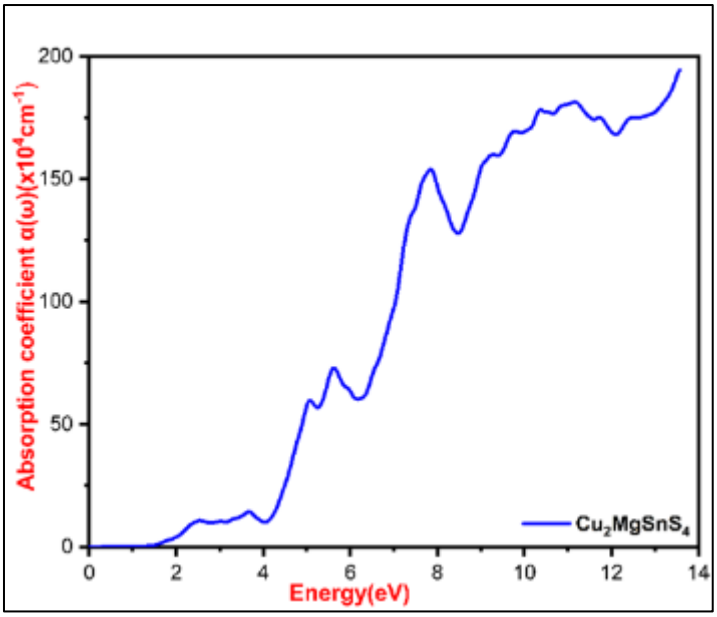

Figure 6 Energy versus absorption coefficient of Cu_2MgSnS_4

The energy loss function provides insight into the electronic mobility within the material. Fig.7 illustrates the energy loss function for Cu_2MgSnS_4, demonstrating the extent of energy dissipation during electronic transitions.

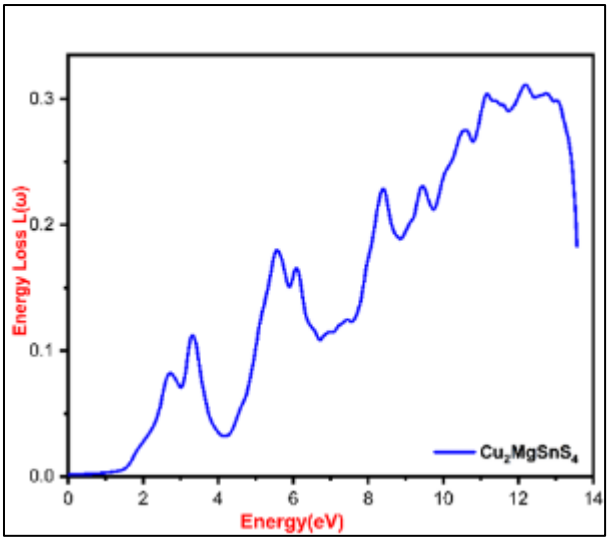

Figure 7 Energy versus energy-loss function of Cu_2MgSnS_4

Additionally, the refractive index characterizes the interaction of photons with the material and the dispersion of incident light**.** The refractive index of the investigated materials is plotted in Figure 8. When its value falls between one and two**,** the material exhibits enhanced optical performance in the UV and visible regions**.** Notably, the real part of the complex dielectric function is analogous to the refractive index, further corroborating the material's optical properties.

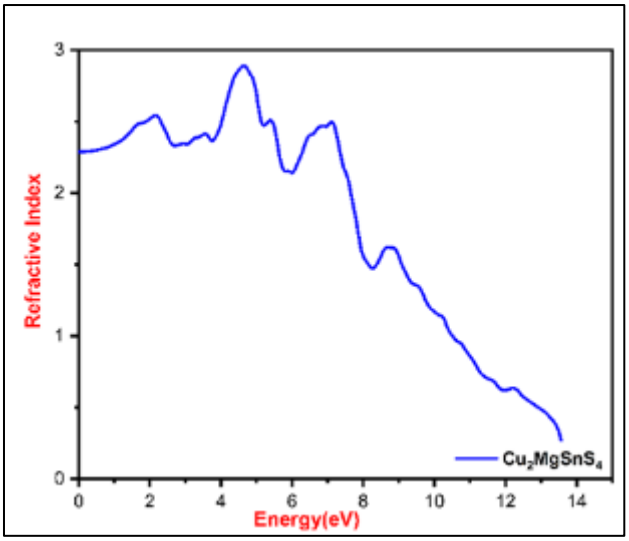

Figure 8 Energy versus Refractive index of Cu_2MgSnS_4

4. Conclusion

In this study, a comprehensive analysis of the ground state properties, electronic structure and optical characteristics of Cu_2MgSnS_4 is presented. Through the application of TB-mBJ+U approximations, it is determined that Cu_2MgSnS_4 exhibit direct band gap. The results of the calculated ground state properties and energy gap values align closely with existing data. Furthermore, the suitable band gaps and high absorption coefficients of Cu_2MgSnS_4 endorse its potential as effective absorber layers in solar cell applications.

References

[1] Suryawanshi MP, Agawane GL, Bhosale SM, Shin SW, Patil PS, Kim JH, Moholkar AV. CZTS based thin film solar cells: a status review. Mater Technol. 2013, 28:98-109.

[2] Li M, Wang T, Xia C, Song G, Chang F. First-principles calculation of electronic structure and optical properties of Cu2ZnSnS4/Cu2ZnSnSe4. Chin J Nonferrous Met. 2012, 22:1413-1420.

[3] Sun KW, Su ZH, Han ZL, Liu FY, Lai YQ, Li J, Liu YX. Fabrication of flexible Cu2ZnSnS4 (CZTS) solar cells by sulfurizing precursor films deposited via successive ionic layer absorption and reaction method. Acta Phys Sin. 2014, 63:018801.

[4] Chen SY, Gong XG, Walsh A, Wei SH. Recent progress in the theoretical study of Cu2ZnSnS4 and related chalcogenide semiconductors. Physics. 2011, 40:248-258.

[5] Siebentritt S, Schorr S. Kesterites - a challenging material for solar cells. Prog Photovolt Res Appl. 2012, 20:512-519.

[6] Katagiri H, Sasaguchi N, Hando S, Hoshino S, Ohashi J, Yokota T. Preparation and evaluation of Cu2ZnSnS4 thin films by sulfurization of E-B evaporated precursors. Sol Energy Mater Sol Cells. 1997, 49:407-414.

[7] Mitzi DB, Gunawan O, Todorov TK, Wang K, Guha S. The path towards a high-performance solution-processed kesterite solar cell. Sol Energy Mater Sol Cells. 2011, 95:1421-1436.

[8] Shin B, Gunawan O, Zhu Y, Bojarczuk NA, Chey SJ, Guha S. Thin film solar cell with 8.4% power conversion efficiency using an earth-abundant Cu2ZnSnS4 absorber. Prog Photovoltaics Res Appl. 2013, 21:72-76.

[9] Winkler MT, Wang W, Gunawan O, Hovel HJ, Todorov TK, Mitzi DB. Optical designs that improve the efficiency of Cu2ZnSn(S,Se)4 solar cells. Energy Environ Sci. 2014, 7:1029-1036.

[10] Ito K, editor. Copper Zinc Tin Sulphide-Based Thin Film Solar Cells. Chichester: John Wiley & Sons, 2015.

[11] Schorr S. Sol Energy Mater Sol Cells. 2011, 95:1482.

[12] Scragg JJS, Larsen JK, Kumar M, Persson C, Sendler J, Siebentritt S, Platzer-Bjorkman C. Phys Status Solidi B. 2016, 253:247.

[13] Chen S, Yang J-H, Gong XG, Walsh A, Wei S-H. Phys Rev B. 2010, 81:245204.

[14] Nagoya A, Asahi R, Wahl R, Kresse G. Phys Rev B. 2010, 81:113202.

[15] Kumar M, Zhao H, Persson C. Thin Solid Films. 2013, 535:318.

[16] Bourdais S, Chon C, Delatouche B, Jacob A, Larramona G, Moisan C, Lafond A, Donatini F, Rey G, Siebentritt S, Walsh A, Dennler G. Adv Energy Mater. 2016, 6:1502276.

[17] Chen L, Deng H, Tao J, Cao H, Huang L, Sun L, Yang P, Chu J. RSC Adv. 2015, 5:84295.

[18] Li L, Liu X, Huang J, Cao M, Chen S, Shen Y, Wang L. Mater Chem Phys. 2012, 133:688.

[19] Zhang X, Bao N, Ramasamy K, Wang YHA, Wang Y, Lin B, Gupta A. Chem Commun. 2012, 48:4956.

[20] Murali B, Madhuri M, Krupanidhi SB. Cryst Growth Des. 2014, 14:3685.

[21] Wang T-X, Li Y-G, Liu H-R, Li H, Chen S-X. Mater Lett. 2014, 124:148.

[22] Kamble A, Mokurala K, Gupta A, Mallick S, Bhargava P. Mater Lett. 2014, 137:440.

[23] Wei M, Du Q, Wang R, Jiang G, Liu W, Zhu C. Chem Lett. 2014, 43:1149.

[24] Wang C, Chen S, Yang JH, Lang L, Xiang HJ, Gong XG, Walsh A, Wei S-H. Chem Mater. 2014, 26:3411.

[25] Zhong G, Tse K, Zhang Y, Li X, Huang L, Yang C, Zhu J, Zeng Z, Zhang Z, Xiao X. Thin Solid Films. 2016, 603:224.

[26] Blaha P, Schwarz K, Madsen GKH, Kvasnicka D, Luitz J, Laskowski R, Tran F, Marks LD. WIEN2k, An Augmented Plane Wave + Local Orbitals Program for Calculating Crystal Properties. Vienna: Techn. Universitat Wien, 2018. ISBN: 3-9501031-1-2.

[27] Blaha P, Schwarz K, Tran F, Laskowski R, Madsen GKH, Laurence D, Marks LD. WIEN2k, An APW+lo program for calculating the properties of solids. J Chem Phys. 2020, 152:07410.

[28] Perdew JP, Burke K, Ernzerhof M. Generalized gradient approximation made simple. Phys Rev Lett. 1997, 77:3865.

[29] Camargo-Martínez JA, Baquero R. Performance of the modified Becke-Johnson potential for semiconductors. Phys Rev B. 2012, 86:195106.

[30] Chen S, Walsh A, Luo Y, Yang J-H, Gong XG, Wei S-H. Wurtzite-derived polytypes of kesterite and stannite quaternary chalcogenide semiconductors. Phys Rev B. 2010, 82:195203.

[31] Murnaghan FD. The compressibility of media under extreme pressures. Proc Natl Acad Sci U S A. 1944, 30:244-247.